High-Resolution Simulations of LS 5039

energetic particles and non-thermal emission

Variable Galactic Gamma-Ray Sources (VII)
Universitat de Barcelona, ICCUB

Ralf Kissmann

Model

Scenario

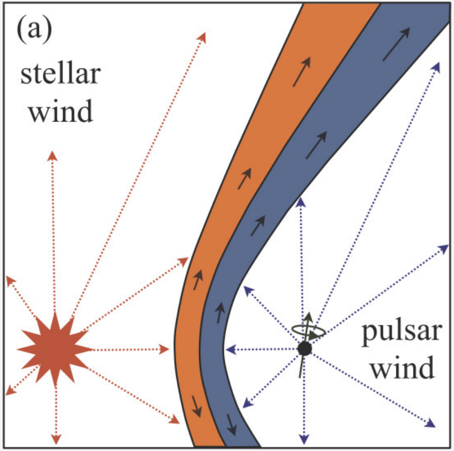

(Dubus (2015))

Wind-Driven Szenario

- Stellar wind
- Pair-plasma outflow from pulsar
- Wind interaction

→ Relativistic Hydrodynamics

Scenario

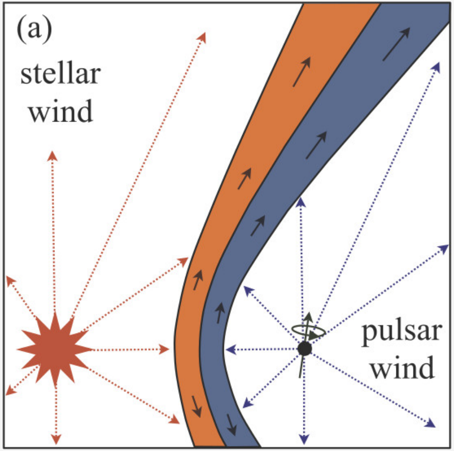

(Dubus (2015))

Wind-Driven Szenario

- Stellar wind
- Pair-plasma outflow from pulsar
- Wind interaction

→ Relativistic Hydrodynamics

Non-thermal Emission

- Purely leptonic model
- Acceleration at shocks of pulsar wind
- Synchrotron & IC
- Pulsar-magnetosphere emission (Takata et al., 2014)

Scenario

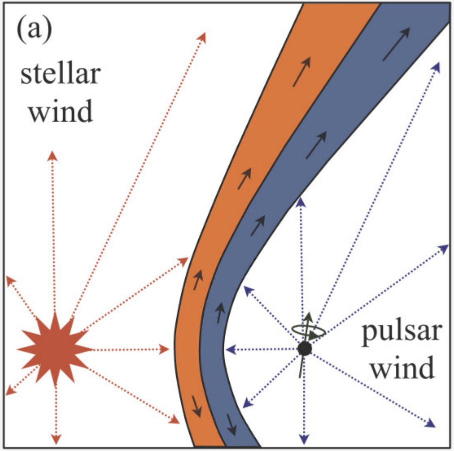

(Dubus (2015))

Numerical Approaches

Example: Semi-Analytical Models

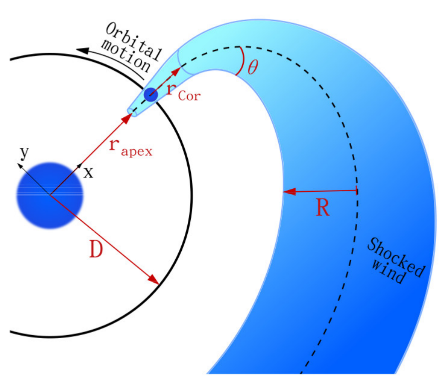

(Molina and Bosch-Ramon (2020))

Numerical Approaches

- Romero et al. (2007), Takata et al. (2012) (classical HD)

Example: Semi-Analytical Models

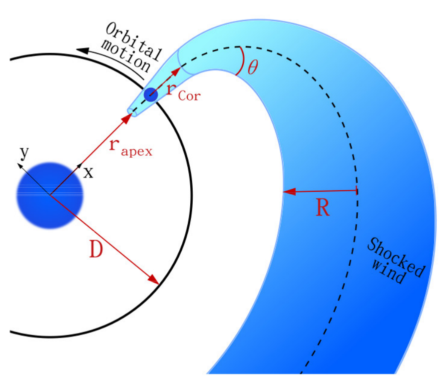

(Molina and Bosch-Ramon (2020))

Modelling Context

Numerical Approaches

- Romero et al. (2007), Takata et al. (2012) (classical HD)
- Bogovalov et al. (2012); Lamberts et al. (2013); Dubus et al. (2015)

Example: Semi-Analytical Models

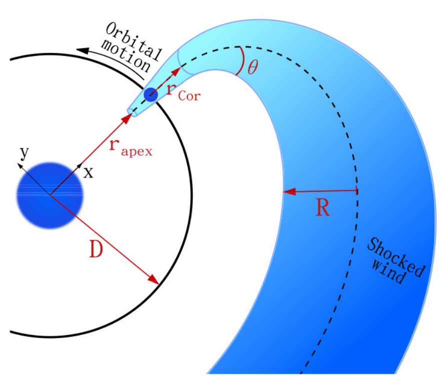

(Molina and Bosch-Ramon (2020))

Numerical Approaches

- Romero et al. (2007), Takata et al. (2012) (classical HD)
- Bogovalov et al. (2012); Lamberts et al. (2013); Dubus et al. (2015)
- Bosch-Ramon et al. (2015) and follow-up studies (3D RHD)

Properties

- full RHD in 3D
- spatially varying resolution

→ large domain

Zoom: Wind-Collision Region

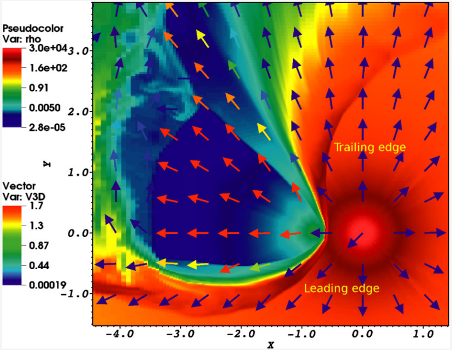

(Bosch-Ramon et al. (2015))

Numerical Approaches

- Romero et al. (2007), Takata et al. (2012) (classical HD)
- Bogovalov et al. (2012); Lamberts et al. (2013); Dubus et al. (2015)
- Bosch-Ramon et al. (2015) and follow-up studies (3D RHD)
- Barkov et al. (2024) (3D RMHD)

Properties

- full RHD in 3D
- spatially varying resolution

→ large domain

Zoom: Wind-Collision Region

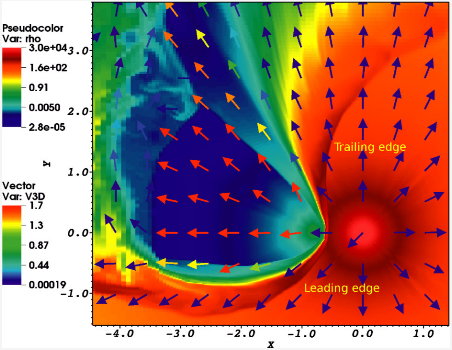

(Bosch-Ramon et al. (2015))

Numerical Approaches

- Romero et al. (2007), Takata et al. (2012) (classical HD)
- Bogovalov et al. (2012); Lamberts et al. (2013); Dubus et al. (2015)
- Bosch-Ramon et al. (2015) and follow-up studies (3D RHD)
- Barkov et al. (2024) (3D RMHD)
- Huber et al. (2021); Kissmann et al. (2023)

Properties

- full RHD in 3D
- homogeneous spatial resolution
- joined with particle transport

Density in Orbital Plane

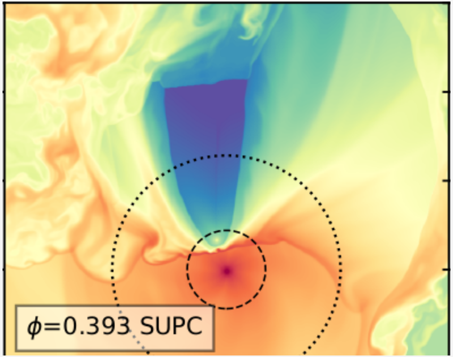

(Huber et al. (2021))

Gas Density

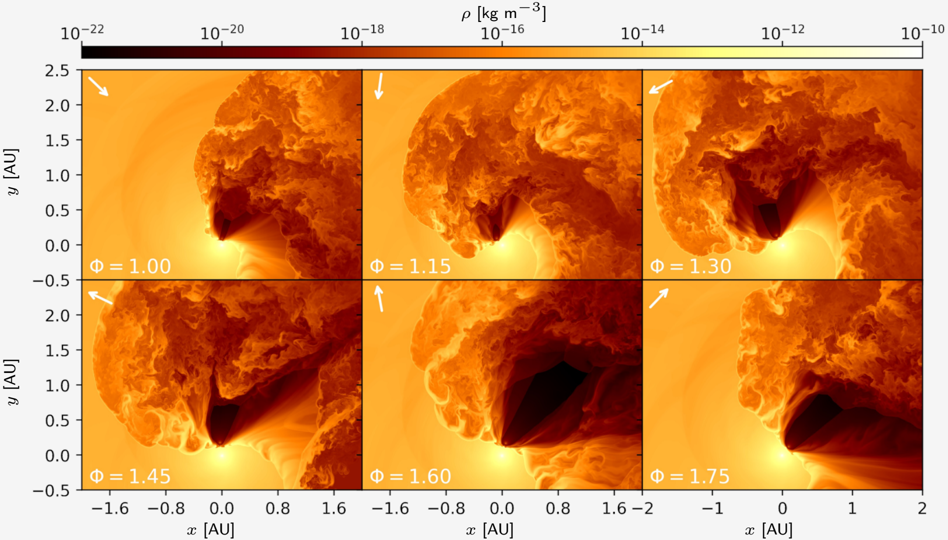

(Kissmann et al. (2023))

Gas Density

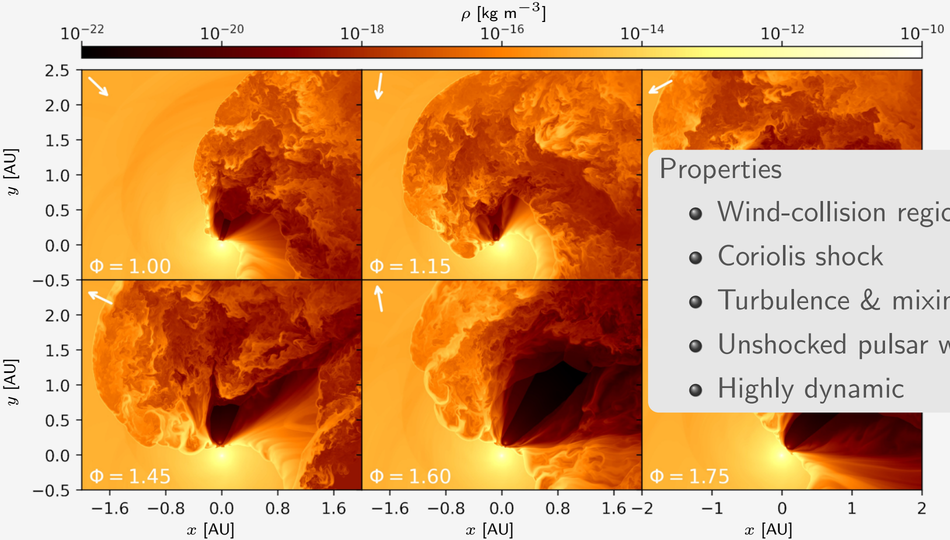

Properties

- Wind-collision region
- Coriolis shock
- Turbulence & mixing
- Unshocked pulsar wind
- Highly dynamic

(Kissmann et al. (2023))

Gas Density

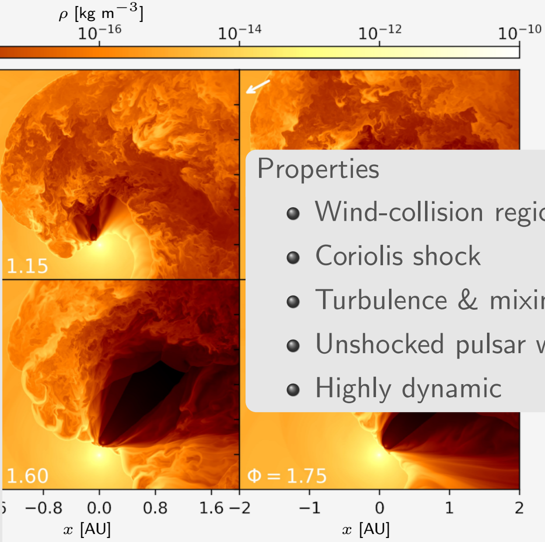

(Kissmann et al. (2023))

Distance of Shocks

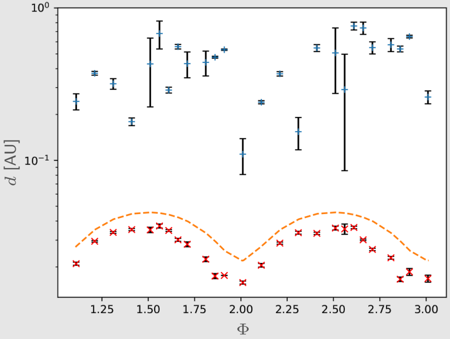

(Kissmann et al. (2023))

Properties

- Wind-collision region
- Coriolis shock
- Turbulence & mixing
- Unshocked pulsar wind
- Highly dynamic

Transport Equation

$$\nabla_\mu \left(u^\mu \mathcal{N}'\right) + \frac{\partial}{\partial \gamma'} \left\{ \left(-\frac{\gamma'}{3} \nabla_\mu u^\mu + \dot{\gamma}'_{rad} \right) \mathcal{N}' \right\} = 0$$

Physical Processes

- Inject spectrum at shocks
  - Maxwellian
  - Power law
  - $\rightarrow$ Tunable parameters
- Transport with fluid flow
- ~~Spatial diffusion~~
- Energy losses

Transport Equation

$$\nabla_\mu \left(u^\mu \mathcal{N}'\right) + \frac{\partial}{\partial \gamma'} \left\{ \left(-\frac{\gamma'}{3} \nabla_\mu u^\mu + \dot{\gamma}'_{rad} \right) \mathcal{N}' \right\} = 0$$

Physical Processes

- Inject spectrum at shocks
  - Maxwellian
  - Power law
  - $\rightarrow$ Tunable parameters
- Transport with fluid flow
- ~~Spatial diffusion~~
- Energy losses

Transport Equation

$$\nabla_\mu \left(u^\mu \mathcal{N}'\right) + \frac{\partial}{\partial \gamma'} \left\{ \left(-\frac{\gamma'}{3} \nabla_\mu u^\mu + \dot{\gamma}'_{rad} \right) \mathcal{N}' \right\} = 0$$

Energy loss processes

- Adiabatic losses
- Synchrotron
- Inverse Compton

Physical Processes

- Inject spectrum at shocks
  - Maxwellian
  - Power law

  $\rightarrow$ Tunable parameters
- Transport with fluid flow
- ~~Spatial diffusion~~
- Energy losses

Transport Equation

$$\nabla_\mu \left(u^\mu \mathcal{N}'\right) + \frac{\partial}{\partial \gamma'} \left\{ \left(-\frac{\gamma'}{3} \nabla_\mu u^\mu + \dot{\gamma}'_{rad} \right) \mathcal{N}' \right\} = 0$$

Energy loss processes

- Adiabatic losses
- Synchrotron
- Inverse Compton

Results

- Position- & energy-dependent particle flux → 4D problem

→ Non-thermal emission

Physical Processes

- Inject spectrum at shocks
  - Maxwellian
  - Power law

  → Tunable parameters
- Transport with fluid flow
- ~~Spatial diffusion~~
- Energy losses

Orbital configuration

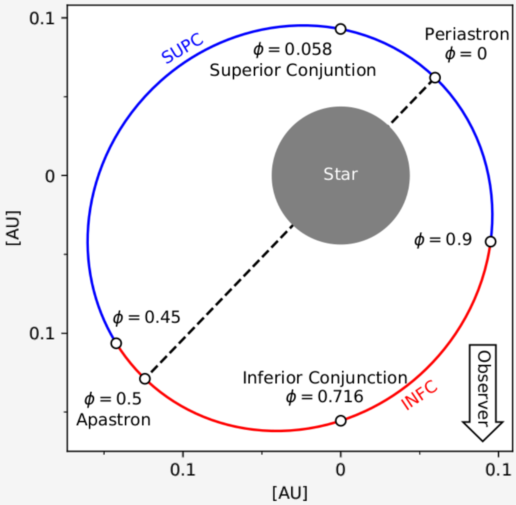

(Huber et al. (2021))

Relevant Numbers

- Numerical domain: 4×3×2 AU
- Spatial resolution: 0.002 AU (2048×1536×1024 cells)
- Energy: $10^8 \ldots 2 \cdot 10^{14}$ eV (30 logarithmic energy bins)
- Co-rotating frame
- Semi-major axis: $a = 0.145$ AU, eccentricity: $e = 0.35$
- Orbital timescale: 3.9 d
- Timestep: $\sim$ 0.5s
- ~10000 cores on Joliot-Curie Rome → 24×10^6 core hours;
- 3 full orbits

Distribution Perpendicular to Orbital Plane

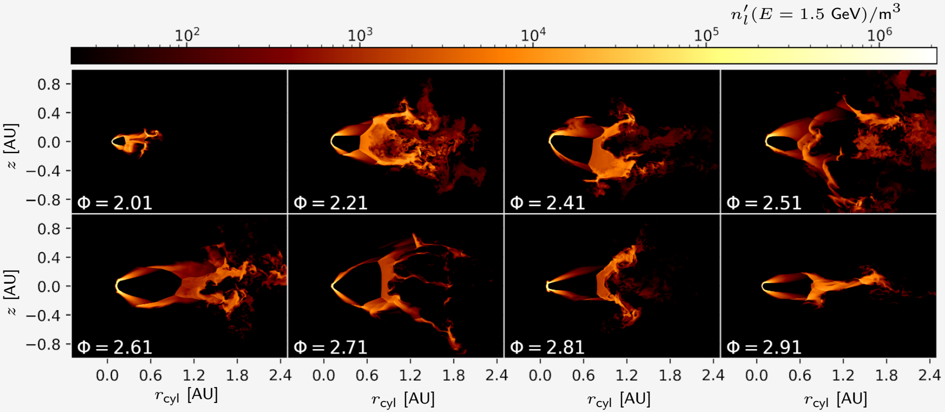

(Kissmann et al. (2025))

Distribution Perpendicular to Orbital Plane

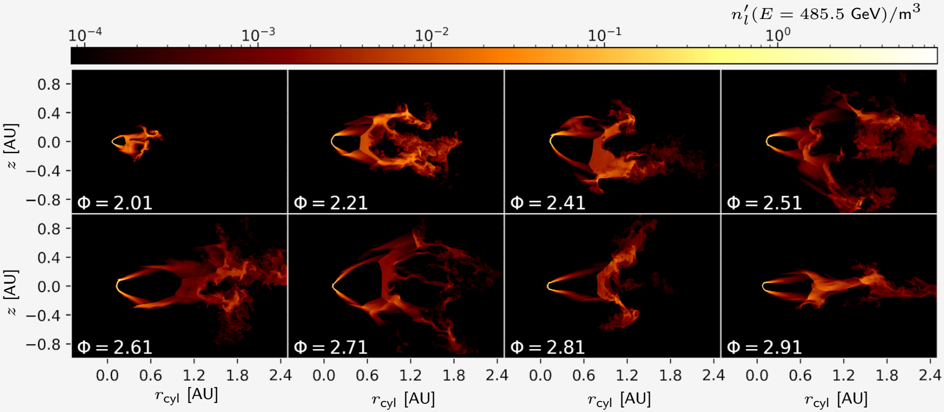

(Kissmann et al. (2025))

Distribution Perpendicular to Orbital Plane

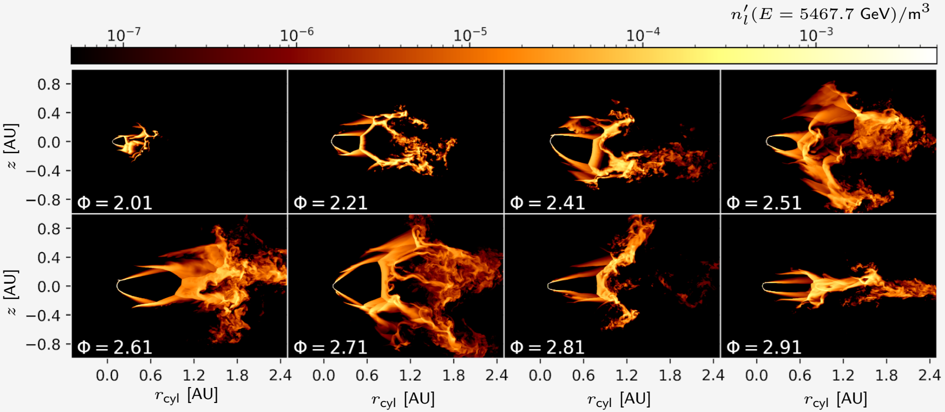

(Kissmann et al. (2025))

Non-Thermal Leptons – Distribution

Distribution Perpendicular to Orbital Plane

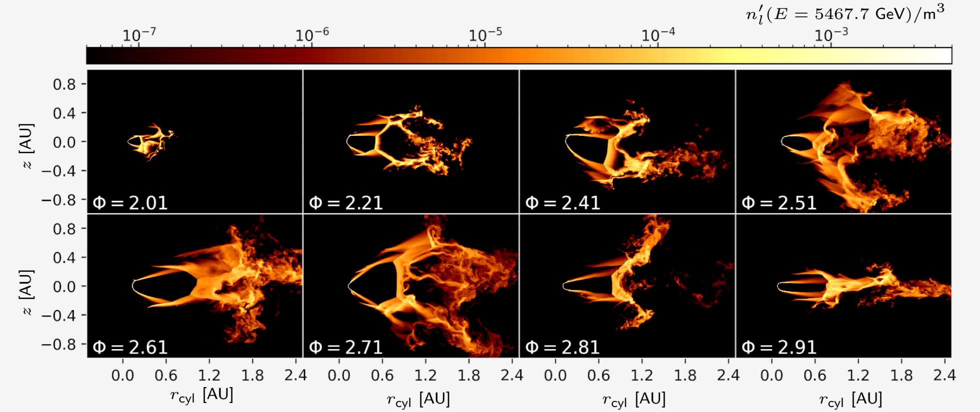

Observations

- Shock thickness
- Energy-loss scale at highest energy
- Suppressed injection at high energy

Non-Thermal Leptons – Distribution

Zoom

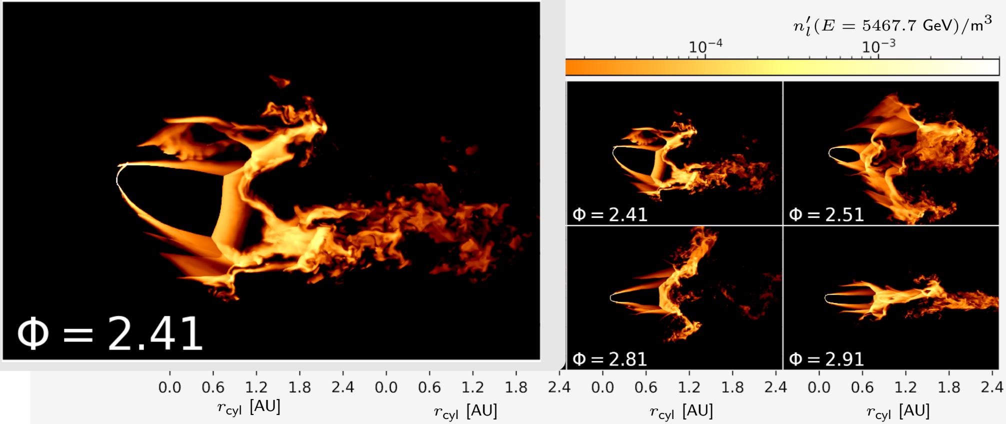

Observations

- Shock thickness
- Energy-loss scale at highest energy
- Suppressed injection at high energy

Spectrum at $\phi = 0.419$

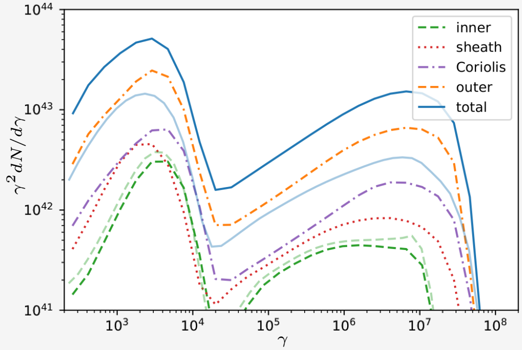

(Kissmann et al. (2025))

Domain-Integrated Particle Spectra

Spectrum at $\phi = 0.419$

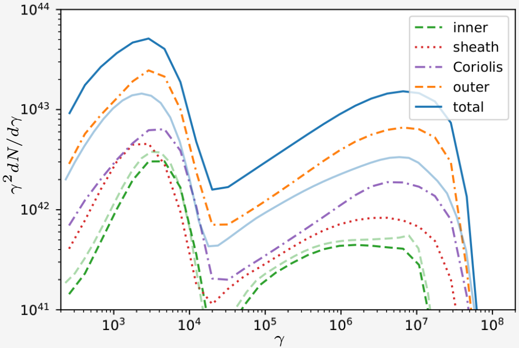

(Kissmann et al. (2025))

Orbital Variation

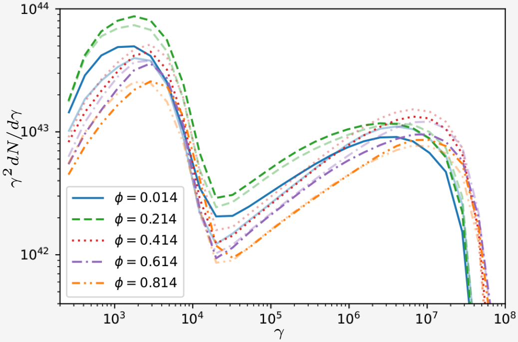

(Kissmann et al. (2025))

Spectrum at $\phi = 0.419$

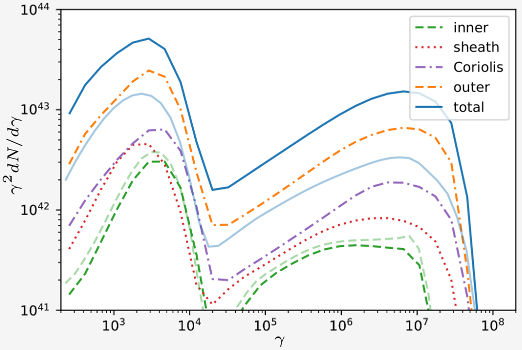

(Kissmann et al. (2025))

Orbital Variation

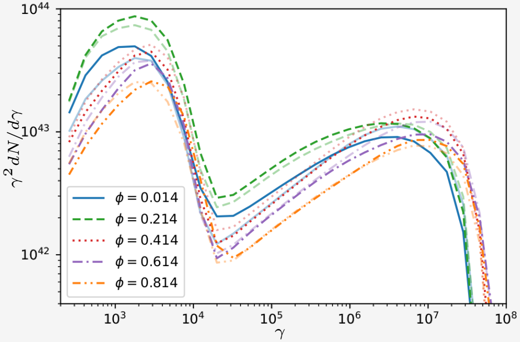

(Kissmann et al. (2025))

Observations

- Power law & transported Maxwellian
- Large number of particles in outer part
- Lower flux & higher energies near apastron

Domain-Integrated Particle Spectra

Spectrum at $\phi = 0.419$

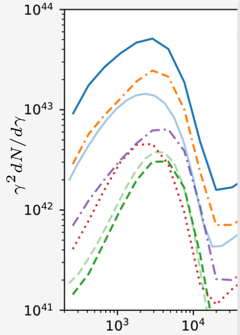

Orbital Variation

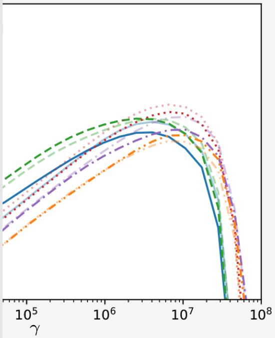

(Kissmann et al. (2025))

Particle Light Curves

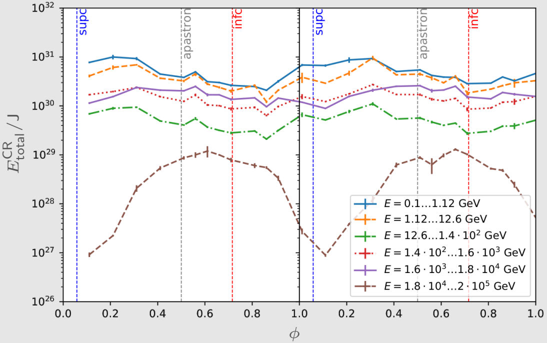

(Kissmann et al. (2025))

Observations

- Power law & transported Maxwellian
- Large number of particles in outer part
- Lower flux & higher energies near apastron

Emission Spectra

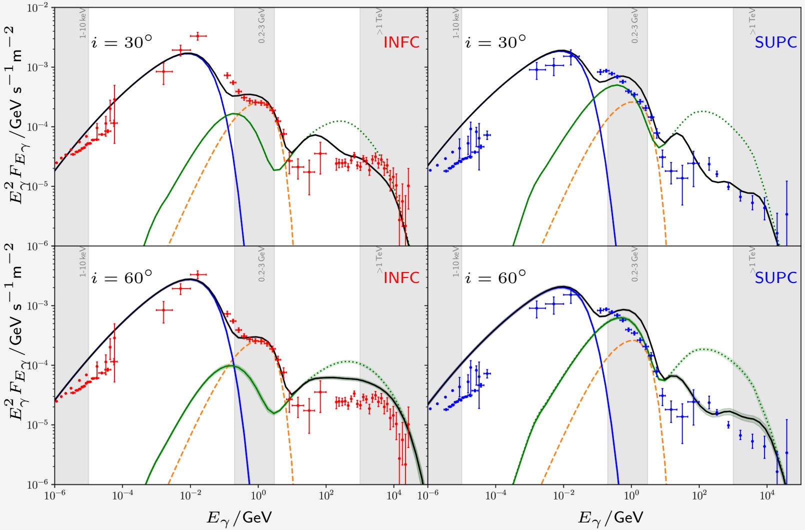

(Kissmann et al. (2025))

Emission Spectra

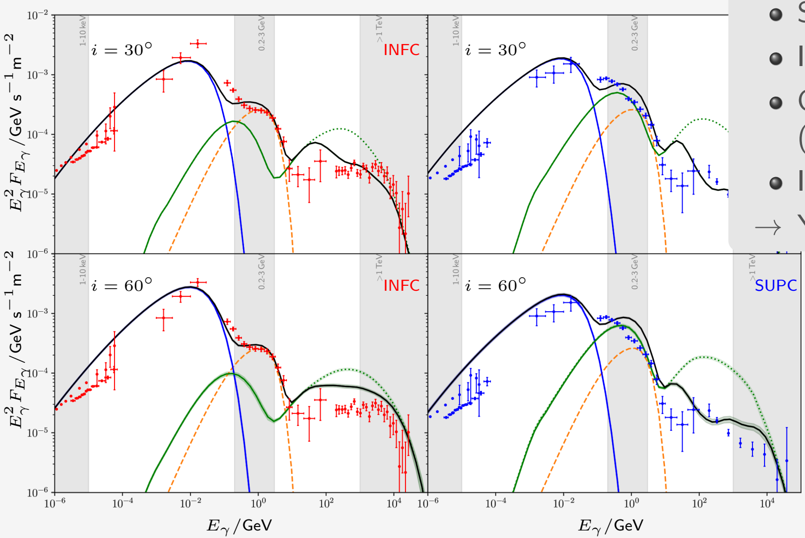

(Kissmann et al. (2025))

Four Components

- Synchrotron
- IC of Maxwellian
- Outer-gap emission (Takata et al., 2014)
- IC of power law

→ Yoneda et al. (2021)

Emission Spectra

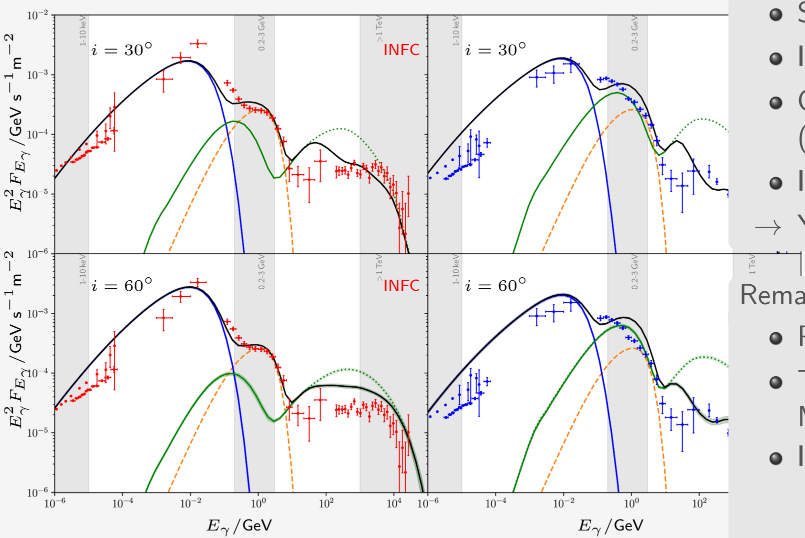

(Kissmann et

Four Components

- Synchrotron
- IC of Maxwellian
- Outer-gap emission (Takata et al., 2014)
- IC of power law

→ Yoneda et al. (2021)

Remarks

- Problems for $i = 60^\circ$
- Transported Maxwellian
- Issues:
  - x-ray regime
  - few GeV regime
- Tuning @low res.

Emission Spectra

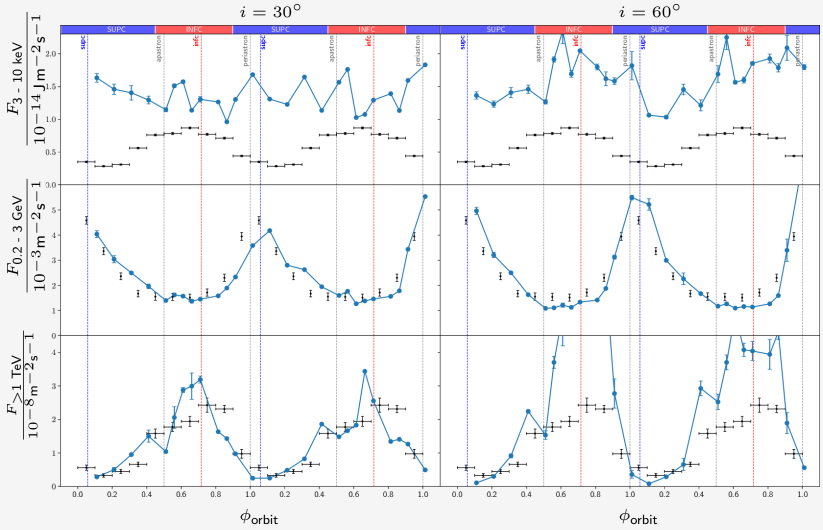

Non-Thermal Emission: Lightcurves

Emission Spectra

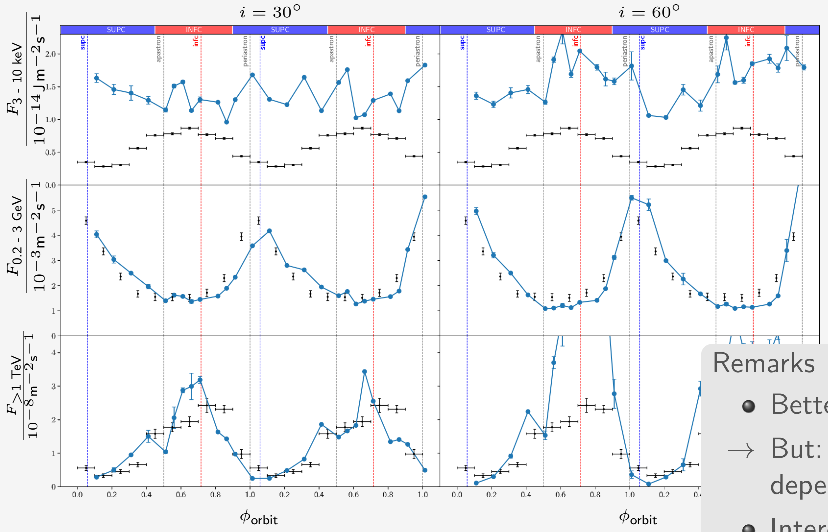

Remarks

- Better fit for $i = 30°$?

$\rightarrow$ But: x-ray phase dependence

- Interesting: trend in x-ray for $i = 60°$?

Modified Flux at Large Inclination?

Modified Spectrum at $i = 60°$

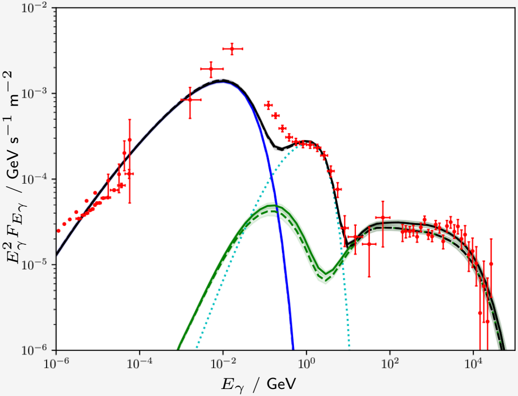

(Kissmann et al. (2025))

Modified Flux at Large Inclination?

Modified Spectrum at $i = 60°$

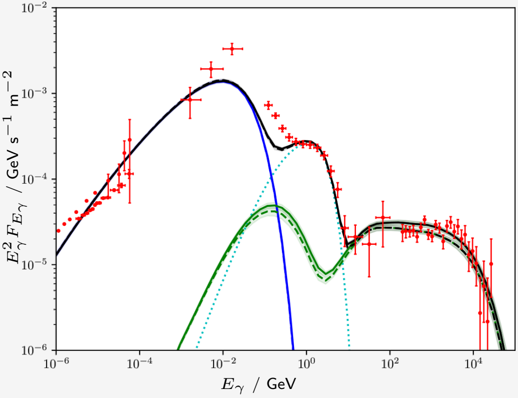

(Kissmann et al. (2025))

Modified Orbital Variation at $i = 60°$

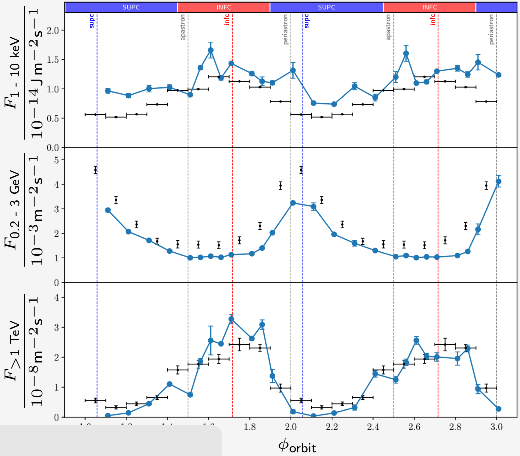

(Kissmann et al. (2025))

Discussion

- Improved GeV regime
- Here: scaling factor 0.5
- But: contribution of Maxwellian

Modified Spectrum at $i = 60°$

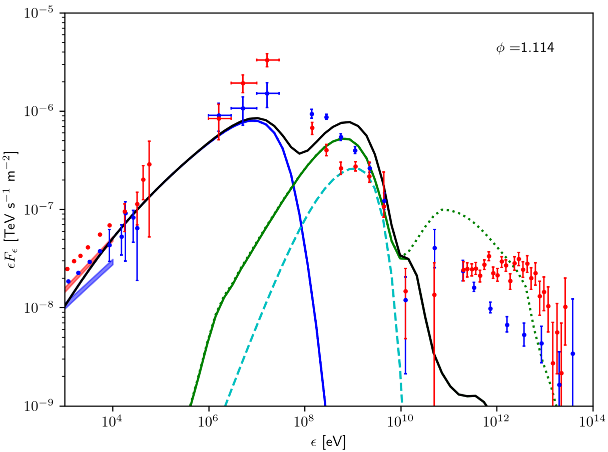

Modified Spectrum at $i = 60°$

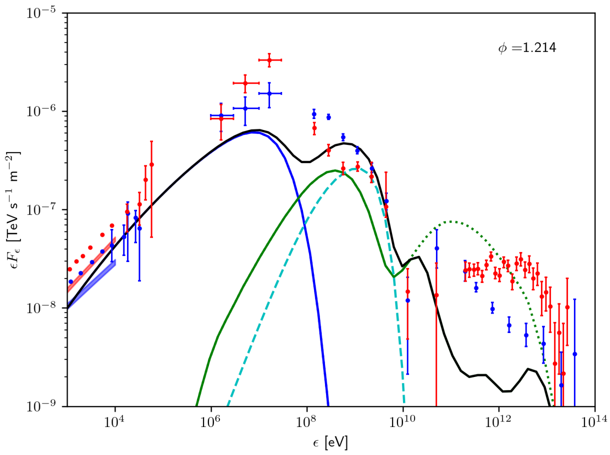

Modified Spectrum at $i = 60°$

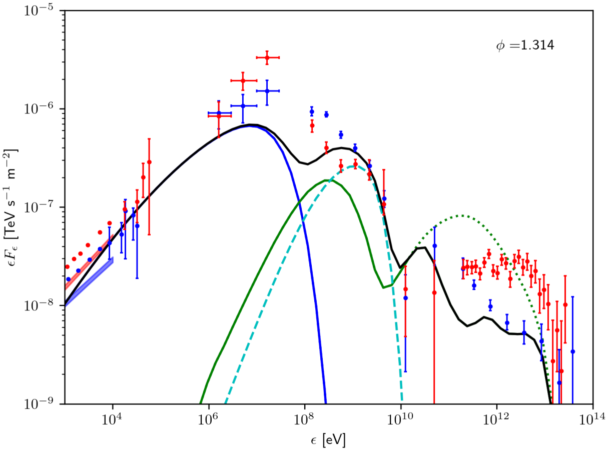

Modified Spectrum at $i = 60°$

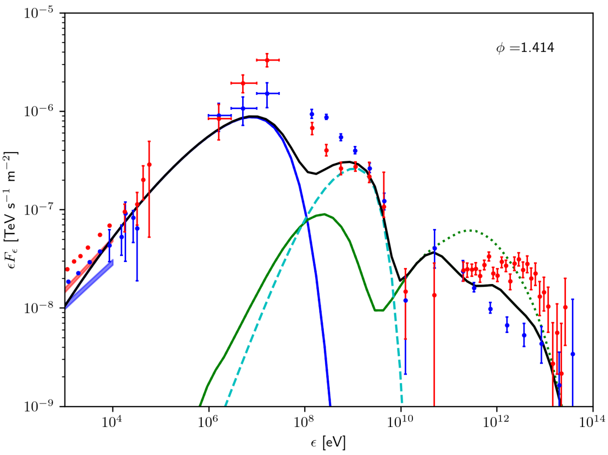

Dynamical Evolution

Modified Spectrum at $i = 60°$

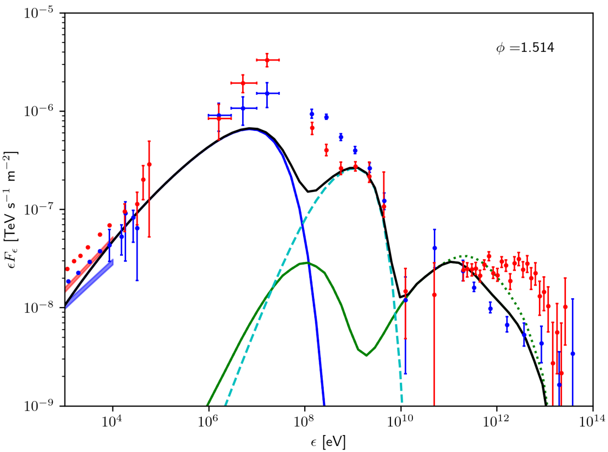

Modified Spectrum at $i = 60°$

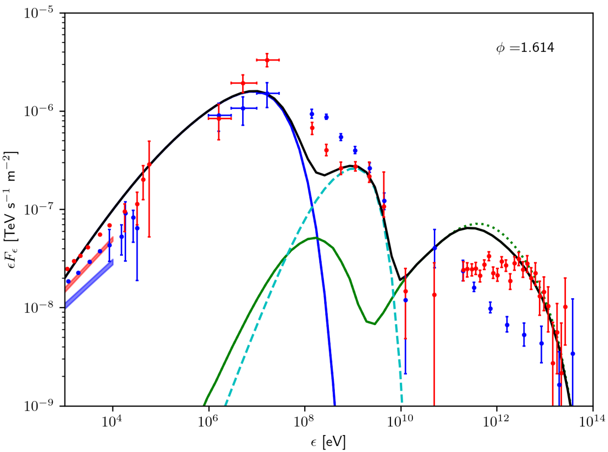

Modified Spectrum at $i = 60°$

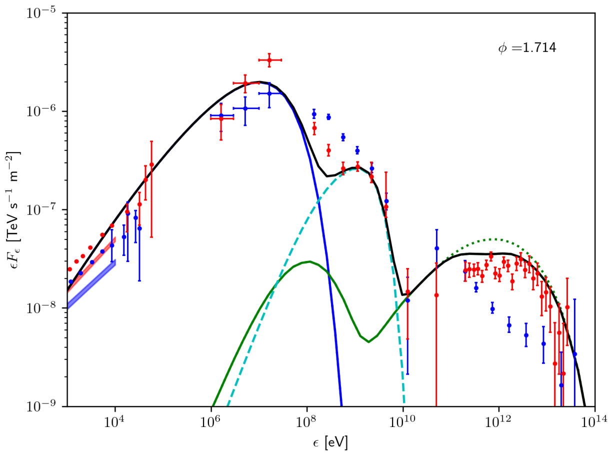

Results: Emission

Modified Spectrum at $i = 60°$

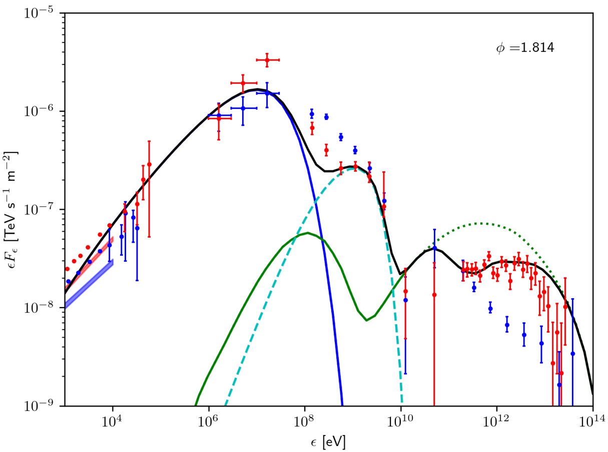

Modified Spectrum at $i = 60°$

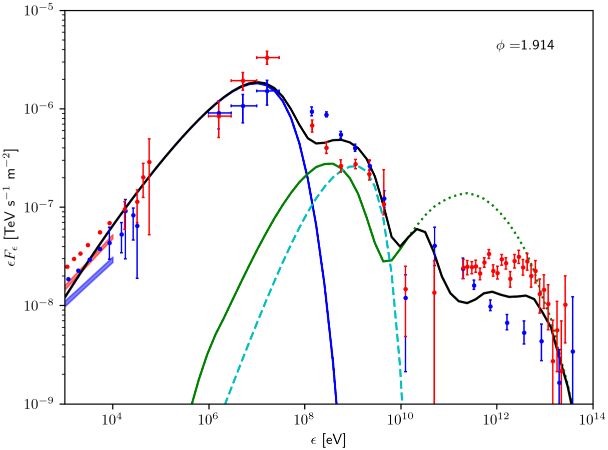

Modified Spectrum at $i = 60°$

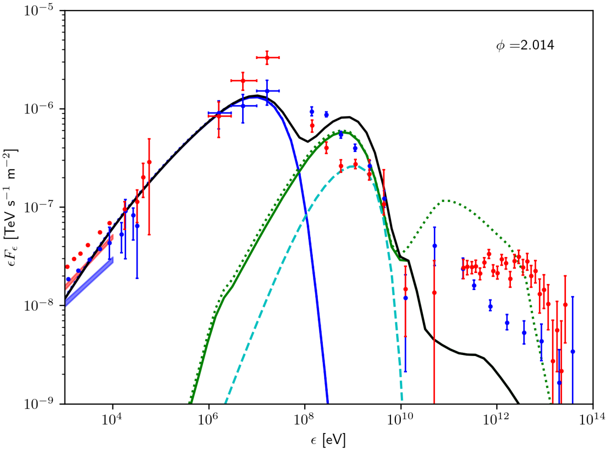

Modified Spectrum at $i = 60°$

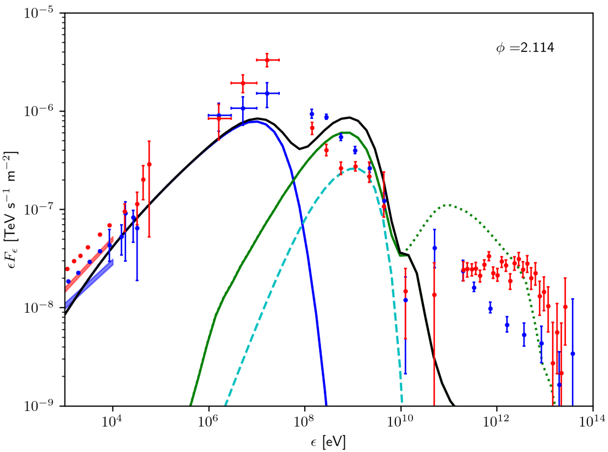

Modified Spectrum at $i = 60°$

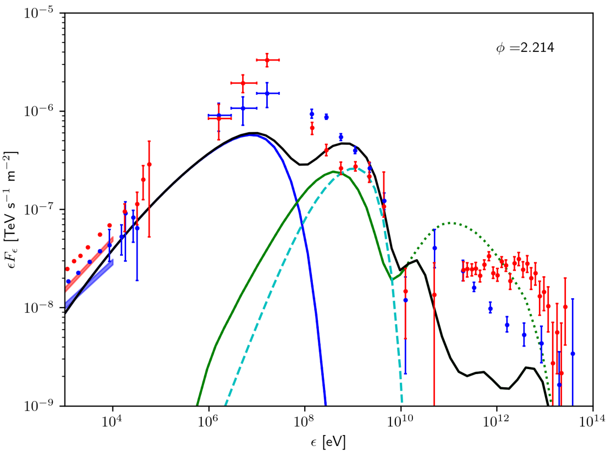

Modified Spectrum at $i = 60°$

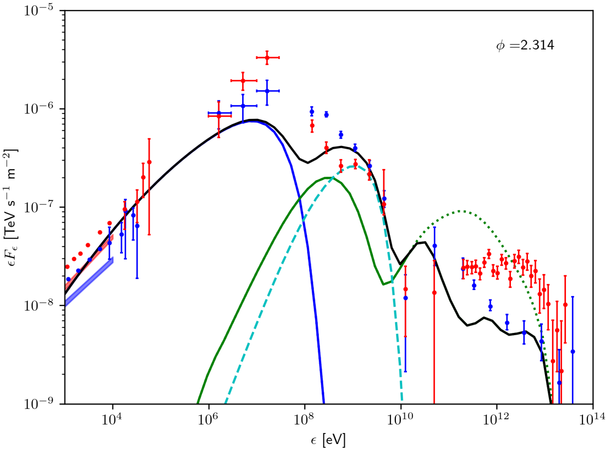

Modified Spectrum at $i = 60°$

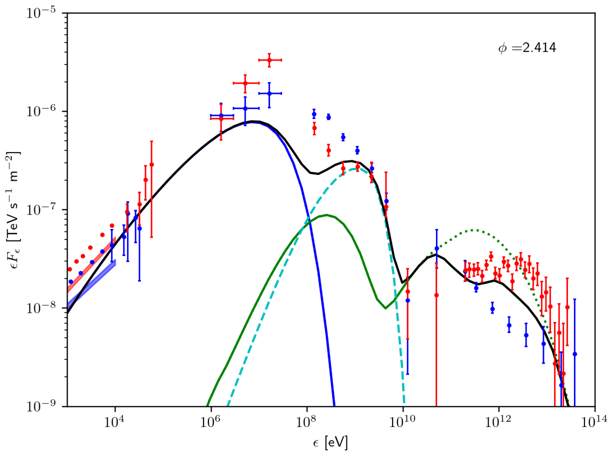

Modified Spectrum at $i = 60°$

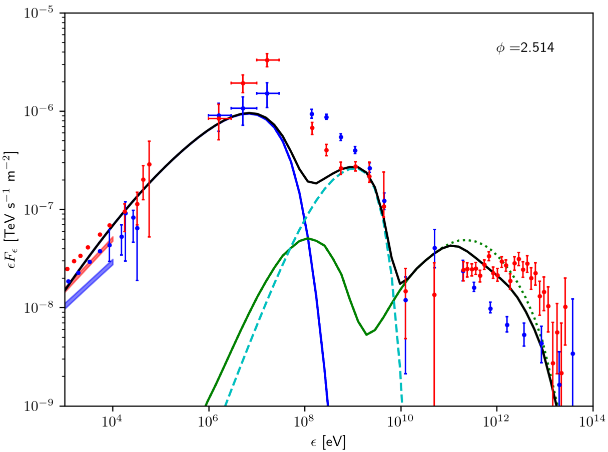

Modified Spectrum at $i = 60°$

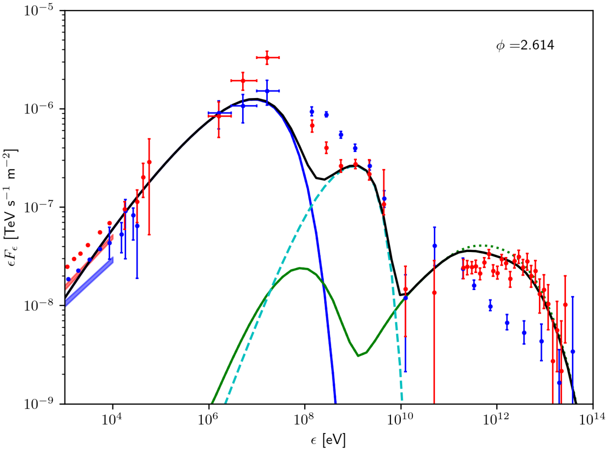

Modified Spectrum at $i = 60°$

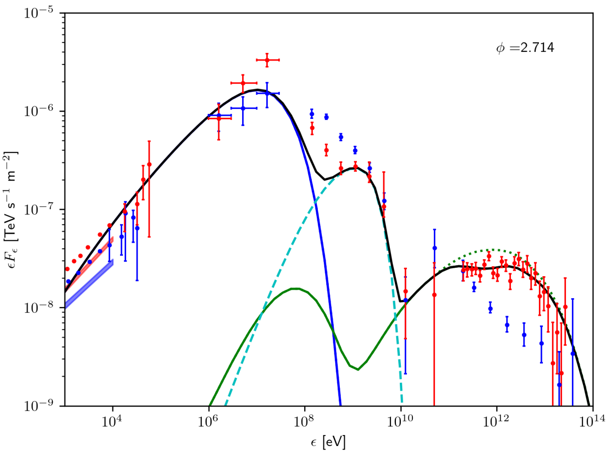

Modified Spectrum at $i = 60°$

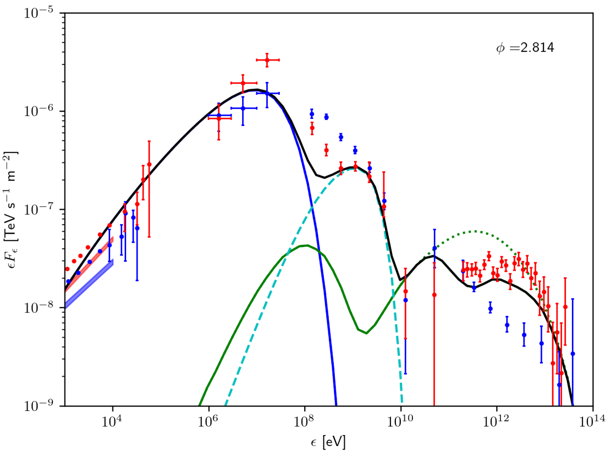

Modified Spectrum at $i = 60°$

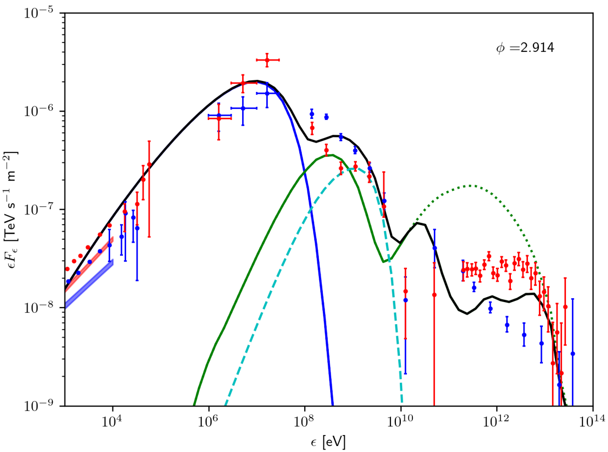

Dynamical Evolution

Modified Spectrum at $i = 60°$

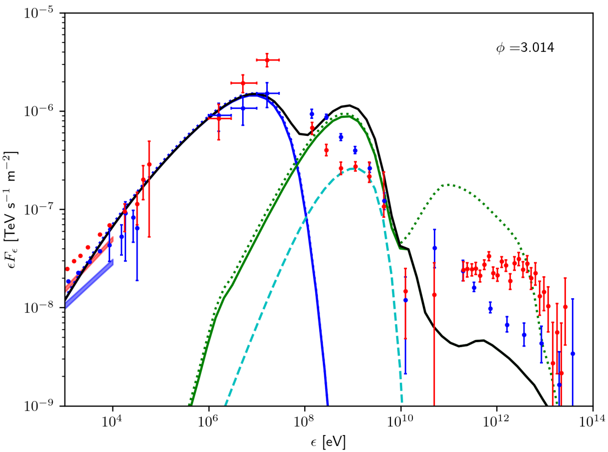

Conclusion

Context

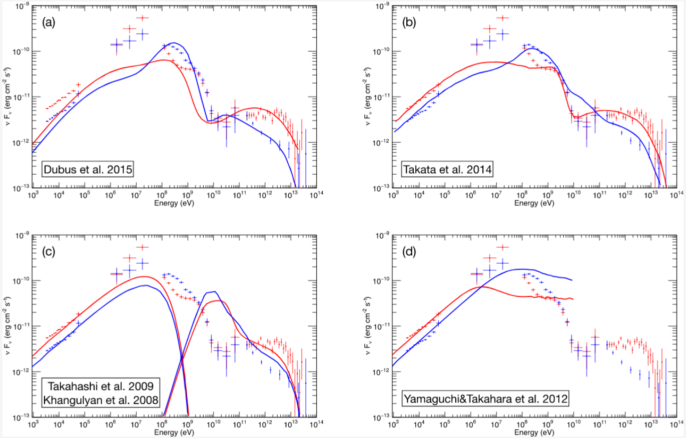

(Yoneda et al. (2021))

Context

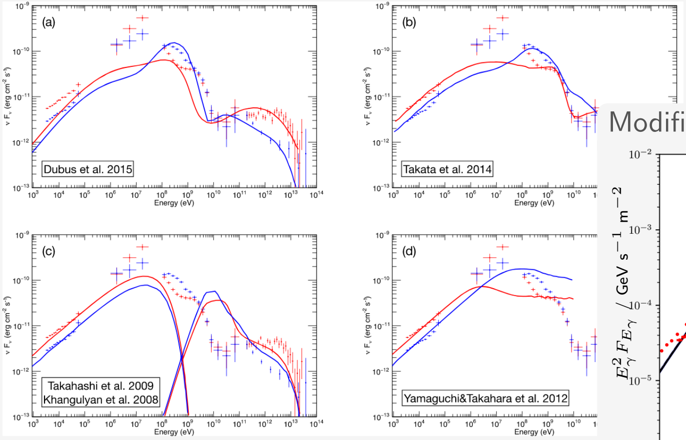

(Yoneda e

Modified Spectrum at $i = 60°$

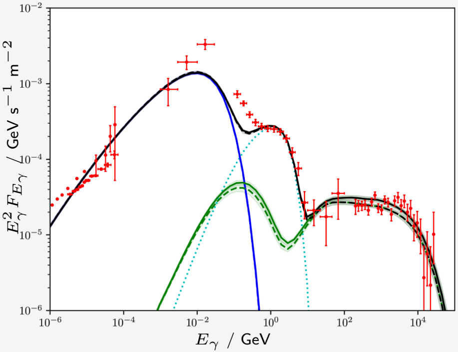

(Kissmann et al. (2025))

Conclusion

Context

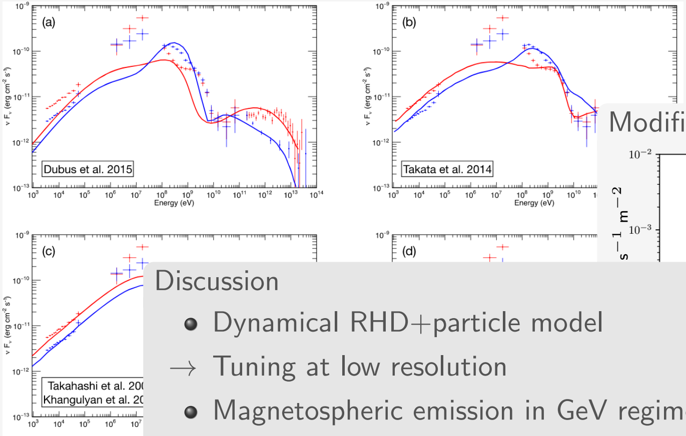

Modified Spectrum at $i = 60°$

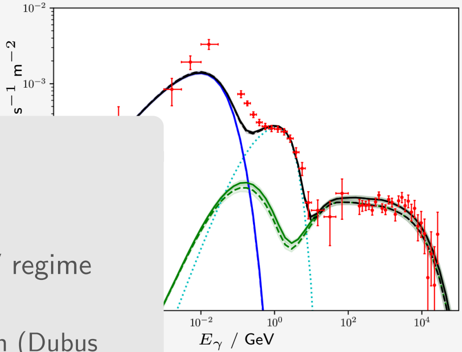

(Kissmann et al. (2025))

Discussion

- Dynamical RHD+particle model

$\rightarrow$ Tuning at low resolution

- Magnetospheric emission in GeV regime
- But:
  - Impact transported Maxwellian (Dubus et al., 2015)
  - x-ray regime $\leftrightarrow$ magnetic-field model
  - UHE gamma rays? (Bykov et al., 2024)

References

Barkov, M., Kalinin, E., and Lyutikov, M. *3D relativistic MHD simulations of the gamma-ray binaries*. PASA, **41**, e048 (2024).

Bogovalov, S. V., et al. *Modelling the interaction between relativistic and non-relativistic winds in the binary system PSR B1259-63/SS2883- II. Impact of the magnetization and anisotropy of the pulsar wind*. MNRAS, **419**(4), 3426 (2012).

Bosch-Ramon, V., Barkov, M. V., and Perucho, M. *Orbital evolution of colliding star and pulsar winds in 2D and 3D: effects of dimensionality, EoS, resolution, and grid size*. A&A, **577**, A89 (2015).

Bykov, A. M., et al. *PeV proton acceleration in gamma-ray binaries*. Advances in Space Research, **74**(9), 4276 (2024).

Dubus, G. *Gamma-ray emission from binaries in context*. Comptes Rendus Physique, **16**, 661 (2015).

Dubus, G., Lamberts, A., and Fromang, S. *Modelling the high-energy emission from gamma-ray binaries usi ng numerical relativistic hydrodynamics*. A&A, **581**, A27 (2015).

Huber, D., Kissmann, R., and Reimer, O. *Relativistic fluid modelling of gamma-ray binaries. II. Application to LS 5039*. A&A, **649**, A71 (2021).

Kissmann, R., Huber, D., and Gschwandtner, P. *High-resolution simulations of LS 5039*. A&A, **677**, A5 (2023).

Lamberts, A., et al. *Simulating gamma-ray binaries with a relativistic extension of RAMSES*. A&A, **560**, A79 (2013).

Molina, E. and Bosch-Ramon, V. *A dynamical and radiation semi-analytical model of pulsar-star colliding winds along the orbit: Application to LS 5039*. A&A, **641**, A84 (2020).

Romero, G. E., et al. *Accretion vs. colliding wind models for the gamma-ray binary LS I +61 303: an assessment*. A&A, **474**, 15 (2007).

Takata, J., et al. *Modeling High-energy Light curves of the PSR B1259-63/LS 2883 Binary Based on 3D SPH Simulations*. ApJ, **750**(1), 70 (2012).

Takata, J., et al. *High-energy Emissions from the Gamma-Ray Binary LS 5039*. ApJ, **790**(1), 18 (2014).

Yoneda, H., et al. *Broadband High-energy Emission of the Gamma-Ray Binary System LS 5039: Spectral and Temporal Features Using NuSTAR and Fermi Observations*. ApJ, **917**(2), 90 (2021).

Distribution in Orbital Plane

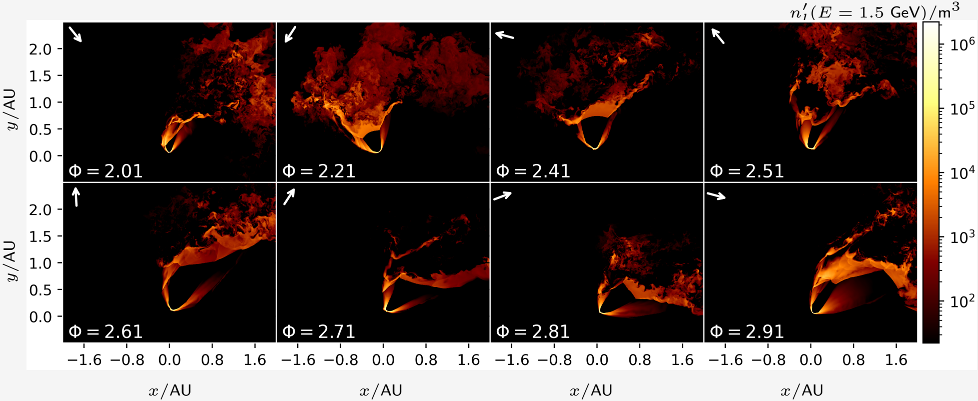

(Kissmann et al. (2025))

Backup: Distributions in Orbital Plane

Distribution in Orbital Plane

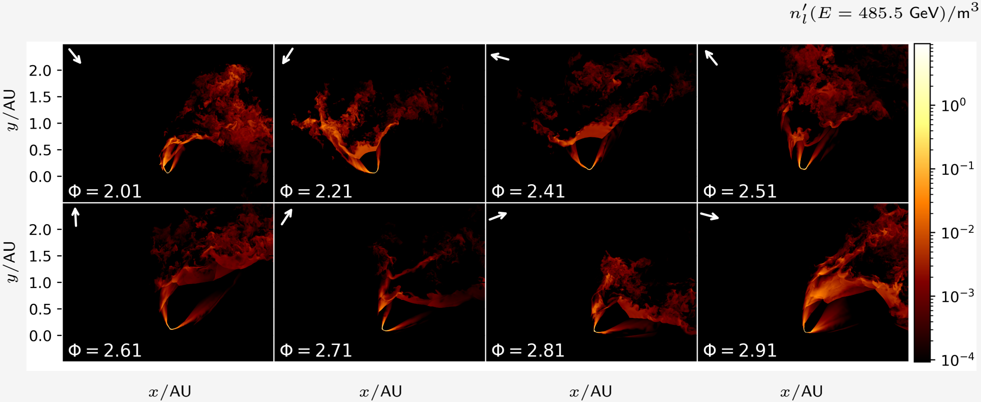

(Kissmann et al. (2025))

Distribution in Orbital Plane

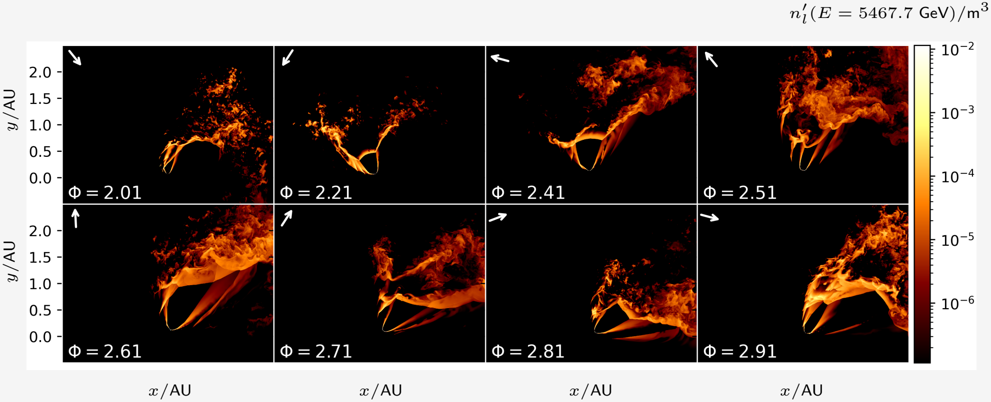

(Kissmann et al. (2025))

Backup: Leptons at Cutoff Energy

Distribution in Orbital Plane

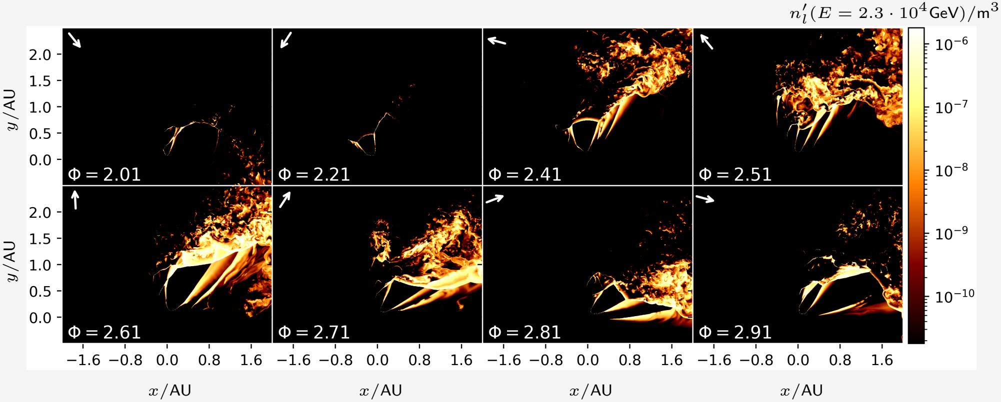

(Kissmann et al. (2025))